Sea Level Measurements along the Alaskan Chukchi and Beaufort Coasts

Principal Investigator
Steve Okkonen
College of Fisheries and Ocean Sciences
University of Alaska Fairbanks

FINAL REPORT
December 2016
OCS Study BOEM 2016-075

BOEM
Bureau of Ocean Energy Management

UAF
University of Alaska Fairbanks

Contact Information:
email: CMI@alaska.edu
phone: 907.474.6782
fax: 907.474.7204

Coastal Marine Institute
School of Fisheries and Ocean Sciences
University of Alaska Fairbanks
P. O. Box 757220
Fairbanks, AK 99775-7220

This study was funded in part by the U.S. Department of the Interior, Bureau of Ocean Energy Management (BOEM) through Cooperative Agreement M14AC00016 between BOEM, Alaska Outer Continental Shelf Region, and the University of Alaska Fairbanks. This report, OCS Study BOEM 2016-075, is available through the Coastal Marine Institute, select federal depository libraries and can be accessed electronically at *http://www.boem.gov/Alaska-Scientific-Publications*.

The views and conclusions contained in this document are those of the authors and should not be interpreted as representing the opinions or policies of the U.S. Government. Mention of trade names or commercial products does not constitute their endorsement by the U.S. Government.

TABLE OF CONTENTS

LIST OF FIGURES iii
LIST OF TABLES iii
INTRODUCTION 1
Objectives 1
METHODS 2
Elson Lagoon Moorings 5
Ancillary Data Sets 7
RESULTS 7
Tidal Height Anomalies 9
Non-Tidal Height Anomalies 12
Elson Lagoon Sea Level and Meade River Freshet 18
CONCLUSIONS 20
ACKNOWLEDGEMENTS 20
STUDY PRODUCTS 20
REFERENCES 21

LIST OF FIGURES

Figure 1. Locations of existing NOAA tide gauges and the communities near pressure sensor deployments 2

Figure 2. Schematic of pressure sensor mooring assembly 3

Figure 3. MODIS satellite image of the Barrow area overlaid with the locations of the Elson Lagoon moorings 5

Figure 4. Billy Adams and Warren Lampe preparing to deploy the sea level recorder mooring at Site 1 in Elson Lagoon near Barrow, Alaska 6

Figure 5. Year-long time series of sea height residuals and temperatures at the three Elson Lagoon sites 8

Figure 6. Year-long time series of 37-constituent composite tidal height anomalies at Red Dog dock, Elson Lagoon sites, and Prudhoe Bay 9

Figure 7. Seasonal variations of semidiurnal tidal amplitudes and phases at Elson Lagoon....11

Figure 8. Year-long time series of non-tidal height anomalies at Red Dog dock, Elson Lagoon sites, and Prudhoe Bay 13

Figure 9. Cross-correlation between winds projected along their axes of variance and non-tidal sea level at Red Dog dock....14

Figure 10. Cross-correlation between winds projected along their axes of variance and non-tidal sea level at Elson Lagoon Site 2 15

Figure 11. Cross-correlation between winds projected along their axes of variance and non-tidal sea level at Prudhoe Bay 16

Figure 12. Meade River discharge and Elson Lagoon non-tidal sea level anomalies, bottom temperatures at mooring sites, and residual heights 19

LIST OF TABLES

Table 1. Mooring locations and deployment/recovery dates 4

Table 2. Amplitudes and phases of the 37 standard tidal constituents at Red Dog dock, Elson Lagoon sites, and Prudhoe Bay....10

Table 3. Lagged cross-correlations between non-tidal sea level anomalies 13

Table 4. Seasonal lagged cross-correlations between non-tidal sea level anomalies 17

INTRODUCTION

Sea level is arguably the most fundamental of oceanographic measurements. Historically, coastal peoples have recognized that changes in sea level can affect travel, commerce, and the exploitation of marine resources; therefore, the ability to understand and predict these changes may greatly improve efficiency and safety in pursuit of these activities. Changes in coastal sea level are caused by ocean currents, storm surges, winds, and tides; causative factors that are not always obvious in the affected region. For example, local observations and recent measurements acquired by current meters in the northern Chukchi and western Beaufort Seas indicate that sea level and coastal currents can change rapidly, even if local winds are calm. These changes are in response to wind-forcing in the southern Chukchi/northern Bering Sea region. These remote winds initiate sea level changes that propagate northward along the Chukchi coast toward Barrow and then eastward along the Beaufort coast (Danielson et al., 2014).

This study was developed in response to questions raised during workshops sponsored by the North Slope Borough-Shell Baseline Studies program (Johnson et al., 2014). Specifically, participants identified information needs relating to relationships among sea level, circulation, and ice movement in coastal areas. With a coastwise separation of nearly one thousand kilometers, long-term NOAA tide gauges (sea level recorders) positioned at Red Dog dock and at Prudhoe Bay are too few and too distant to use effectively in systematically investigating relationships between local sea level and ocean processes along the entire Chukchi-Beaufort coast. This study extended the network of sea level recorders deployed along the Alaskan arctic coast to provide additional sea level data for the region.

Objectives

The objective of this project was to deploy sea level recorders (pressure sensors) to acquire year-long (summer 2014–summer 2015) records of local sea level at Point Hope, Point Lay, Wainwright, Barrow, and Kaktovik (Figure 1). These measurements, along with those acquired by NOAA gauges at Red Dog and Prudhoe Bay, were intended to address the specific goals of:

1) Improving our understanding of ocean circulation and improving computer models of ocean circulation in the Chukchi and Beaufort Seas;

2) Investigating relationships between landfast ice breakout events and sea level changes;

3) Assessing the effects of sea level changes on coastal erosion; and

4) Obtaining data to inform coastal protection and engineering design issues.

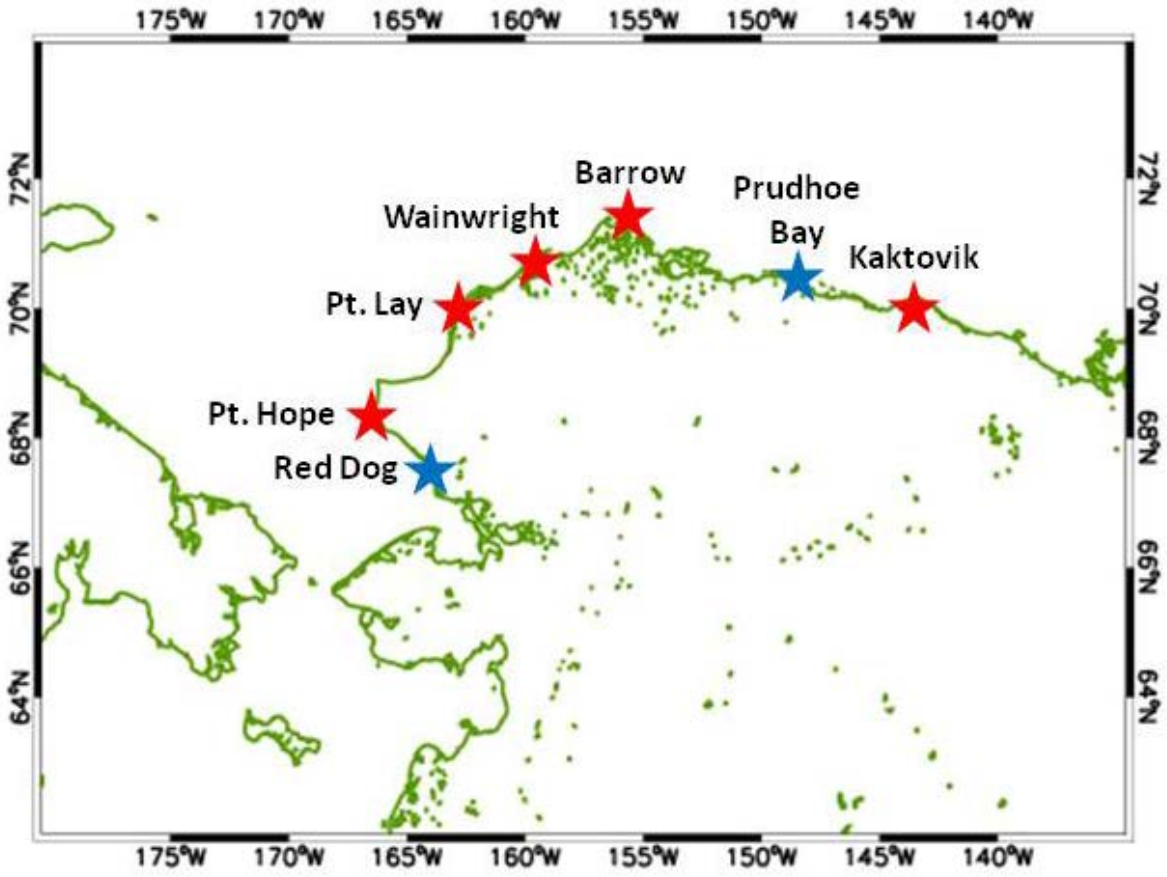

Figure 1: Locations of existing NOAA tide gauges (blue stars) and the communities near pressure sensor deployments (red stars).

METHODS

Fifteen simple moorings were deployed for this project; three near each of the five participating communities. Moorings were instrumented with either RBRduo T.D or Onset HOBO U20-001-01 pressure/temperature sensors. Both pressure sensor models have full-scale accuracies of at +/- 1.0 hPa, or better, and full-scale resolutions of <0.2 hPa. Based on the hydrostatic equation and typical estuarine sea water densities (1000 kg m^{-3} < ρ < 1030 kg m^{-3}), these pressure values are very nearly numerical equivalents to water level accuracy and resolution in centimeters (i.e., ~1 cm and ~0.2 cm, respectively). The accuracy and resolution of the RBRduo temperature sensor, +/- 0.002°C and <0.00005°C, respectively, were much better than the corresponding values for the Onset sensor, +/- 0.44°C and 0.10°C. The RBRduos acquired pressure and temperature measurements at 5-minute intervals. Three Onset sensors, having smaller internal memories, were programmed to acquire measurements at 30-minute intervals. The 5-minute RBRduo data were subsampled at 30-minute intervals for direct comparison with the Onset data.

Each mooring was comprised of a pressure sensor attached to a plastic base plate secured to a cement pier block. This assembly was then connected to a second pier block using eyebolts and a

50-ft (15-m) Kevlar ground line to facilitate recovery of the mooring assembly using a grappling hook (Figure 2).

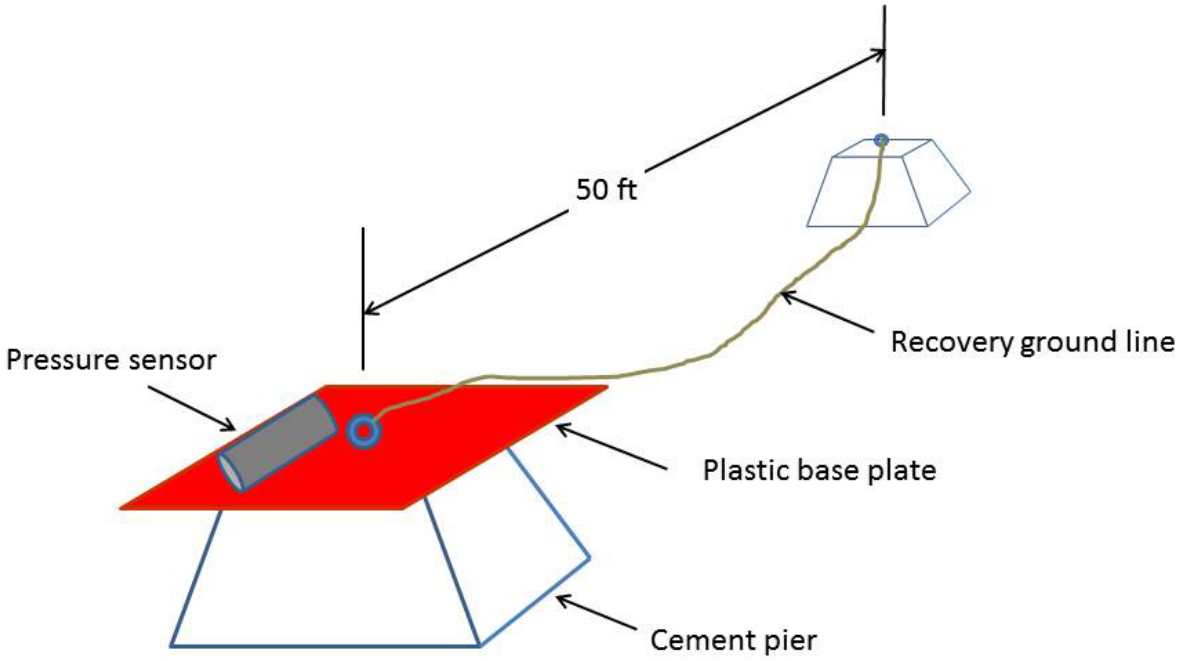

Figure 2: Schematic of pressure sensor mooring assembly.

Three moorings were deployed in lagoons or protected waters near the sentinel communities. Each site included a primary mooring, instrumented with an RBRduo, and two secondary moorings instrumented with Onsets. Local crews identified sight locations and depths where the potential for instrument loss or damage due to ice scouring was believed to be least likely. Each of the primary moorings was deployed as close as practical to the principal passage connecting the open ocean to the lagoon or protected embayment. The secondary moorings were deployed at more distant locations but near minor passages where possible. At each mooring site (Table 1), GPS location was recorded and the pressure/temperature sensor pier block was lowered to the bottom using the recovery ground line. The second (recovery) pier block was dropped ~50 feet away.

Due to whaling activities and other conflicts, only moorings deployed near Barrow in Elson Lagoon were recovered in fall 2015; recoveries were not attempted at the other community sites in fall 2015. Attempts to recover the moorings deployed at Point Lay and Kaktovik in fall 2016 were unsuccessful.

Table 1: Mooring locations and deployment/recovery dates.

Community	Location	Sensor Type	Deployed / Recovered
Point Hope	68° 25.060’ N 166 24.529’ W	RBRduo	In: 6 September 2014 NOT RECOVERED
	68° 25.115’ N 166° 23.959’ W	Onset	In: 6 September 2014 NOT RECOVERED
	68° 25.095’ N 166° 23.555’ W	Onset	In: 6 September 2014 NOT RECOVERED
Point Lay	69° 53.821’ N 162° 49.765’ W	RBRduo	In: 4 September 2014 NOT RECOVERED
	69° 39.831’ N 163° 06.767’ W	Onset	In: 4 September 2014 NOT RECOVERED
	69° 24.803’ N 163 08.235 W	Onset	In: 4 September 2014 NOT RECOVERED
Wainwright	70° 35.023’ N 160° 06.757’ W	RBRduo	In: 21 August 2014 NOT RECOVERED
	70° 35.636’ N 160° 01.416’ W	Onset	In: 21 August 2014 NOT RECOVERED
	70° 34.786’ N 159° 53.199’ W	Onset	In: 21 August 2014 NOT RECOVERED
Barrow	71° 21.420’ N 156° 21.797’ W	RBRduo	In: 20 August 2014, 1000 UTC Out: 21 September 2015, 2140 UTC
	71° 15.026’ N 156° 0.013’ W	Onset	In: 7 September 2014, 0200 UTC Out: 21 September 2015, 2200 UTC
	71° 11.416’ N 155° 34.710’ W	Onset	In: 7 September 2014, 0300 UTC Out: 22 September 2015, 1930 UTC
Kaktovik	70° 08.232’ N 143° 35.273’ W	RBRduo	In: ~8–12 September 2014 NOT RECOVERED
	70° 07.419’ N 143° 34.690’ W	Onset	In: ~8–12 September 2014 NOT RECOVERED
	70° 07.706’ N 143° 34.102’ W	Onset	In: ~8–12 September 2014 NOT RECOVERED

Elson Lagoon Moorings

Sensor moorings were deployed at three locations along Elson Lagoon (Figure 3, Figure 4, and Table 1), with Sites 1 and 3 being separated by ~34 km. The Site 1 RBRduo was deployed at a depth of ~4.2 meters near a small bight at the end of the spit adjacent to Eluitkak Pass (Nuvugaluak). This site was largely sheltered from wind-induced waves and their associated pressure signals. In contrast, Onset sensors at Sites 2 and 3 were deployed at exposed locations more than 1 km from shore and at shallower depths of ~2.4 and ~2.9 meters, respectively. These sensors recorded pressure signals associated with wind-induced waves.

Figure 3: MODIS satellite image of the Barrow area overlaid with the locations of the Elson Lagoon moorings (red diamonds). Meade River discharges into Admiralty Bay.

While the pressure/temperature sensors in Elson Lagoon had slightly different deployment histories, the deployment periods overlapped from 0300 UTC, 7 September 2014 through 2130 UTC, 21 September 2015 (Table 1). Ignoring partial-day data from the beginning and end of this concurrent sampling period, data acquired at the three locations between 0000 UTC, 8 September 2014 and 2330 UTC, 20 September 2015 were adopted as the working data set; the 378-day duration being sufficient to resolve all 37 standard tidal harmonic constituents.

Figure 4: Billy Adams (left) and Warren Lampe (right) preparing to deploy the sea level recorder mooring at Site 1 in Elson Lagoon near Barrow, Alaska.

The pressure time series recorded by the RBRduo and Onset sensors include pressure contributions from the atmosphere and water column as follows:

$$P_{total}(t) = P_{atm}(t) + P_{water}(t) \qquad \text{Equation 1}$$

The water column pressure record, obtained after subtracting the NCEP sea level pressure from the total pressure record, is comprised of time-varying tidal and non-tidal signals superimposed on a fixed pressure, P_0, attributable to the mean depth of the water column:

$$P_{water}(t) = P_{tide}(t) + P_{non-tide}(t) + P_0 \qquad \text{Equation 2}$$

The composite tidal signal, P_{tide}, was estimated using a least squares procedure to fit the 37 standard tidal harmonic constituents (Table 2) to the time series of water column pressures:

$$P_{tide}(t) = \sum_{i=1}^{37} P_i \cos(\omega_i t + \phi_i) \qquad \text{Equation 3}$$

Here, t is the time in hours relative to 0000UTC, 1 January 2014, and P_i, ω_i, and ϕ_i are the amplitude, angular frequency, and phase lag of tidal constituent i .

Given the water column pressure, computed estimate of the tidal signal, and mean pressure of the water column, the non-tidal pressure signal is readily obtained from manipulation of equation 2. As noted, pressures in hPa are very nearly numerical equivalents to sea level heights (in centimeters) for the range of sea water densities and shallow depths in Elson Lagoon. Accordingly, pressures and pressure changes will, hereafter, be characterized as sea level heights or height anomalies.

Ancillary Data Sets

Hourly sea level data from NOAA tide gauges at Red Dog Dock and Prudhoe Bay were obtained from NOAA (http://tidesandcurrents.noaa.gov/stations.html?type=Historic+Water+Levels). Hourly data corresponding to the 378-day Elson Lagoon sensor records were interpolated to 30-minute intervals for comparison with Elson Lagoon sea level (pressure) and Barrow Canyon ocean current data sets.

Time series of sea level atmospheric pressures and surface winds were obtained from NOAA 2.5° x 2.5° NCEP/NCAR Reanalysis 1, 4-times daily (0Z, 6Z, 12Z, 18Z) data sets (http://www.esrl.noaa.gov/psd/data/gridded/data.ncep.reanalysis.surface.html). Sea level pressures from the four NCEP grid points surrounding Barrow (70.0°N,157.5°W; 70.0°N, 155.0°W; 72.5°N,157.5°W; 72.5°N, 155.0°W) were averaged at each 6-hour time step. The 6-hourly atmospheric pressure data were interpolated to 30-minute intervals and subtracted from the raw mooring pressure data to obtain water column pressure. The 6-hourly wind data were used in correlation analyses with sea level data that were subsampled at 6-hour intervals.

A time series of Meade River discharge was obtained from the US Geological Survey Alaska streamflow website (http://waterdata.usgs.gov/ak/nwis/current/?type=flow). The only available 2015 data were for the period from 23 May to 6 June.

RESULTS

In some respects, two seasons characterize Arctic Alaska's coastal marine environment: an open-water season and an ice-covered season. As shown below, sea level in Elson Lagoon and its response to local and remote forcing are largely defined by these two seasons. Water temperature is an obvious measurement by which these two seasons might be identified. Temperature data (Figure 5, bottom panel) suggest that freeze-up occurs sometime around mid-September. The jump in temperature to ~0°C in late May, indicative of the onset of the spring freshet, might be interpreted as signaling breakup. However, sea level time series, $H_{water}\ (t)$, provide another means to reasonably identify the dates of freeze-up and breakup in Elson Lagoon and, thereby, differentiate the seasons.

Because sea ice dampens surface waves, sea level measurements acquired during the open-water season should be noisier than sea level measurements acquired during the ice-covered season. This concept is simply illustrated by time series of the difference between raw sea level measurements and smoothed (3-point, 1.5-hour boxcar) sea level measurements at each mooring site (Figure 5). These residual heights are, therefore, proxies for open-water and ice-covered seasons. The time series residuals at Site 1 are generally small (< ~2 cm) during the summer months, likely attributable to the site's more protected location, and during the winter months as well due to ice cover. As such, it is difficult to identify open-water and ice-covered seasons. In contrast, there are two reasonably well-defined residual height modes at Sites 2 and 3. Using a somewhat subjective characterization of seasons based on the residual time series at these two

sites, forthcoming analyses will refer to the period from 8 September –13 October 2014 as the fall open-water season, the period from 14 October 2014–13 June 2015 as the winter ice-covered season, and the period from 14 June–20 September 2015 as the summer open-water season.

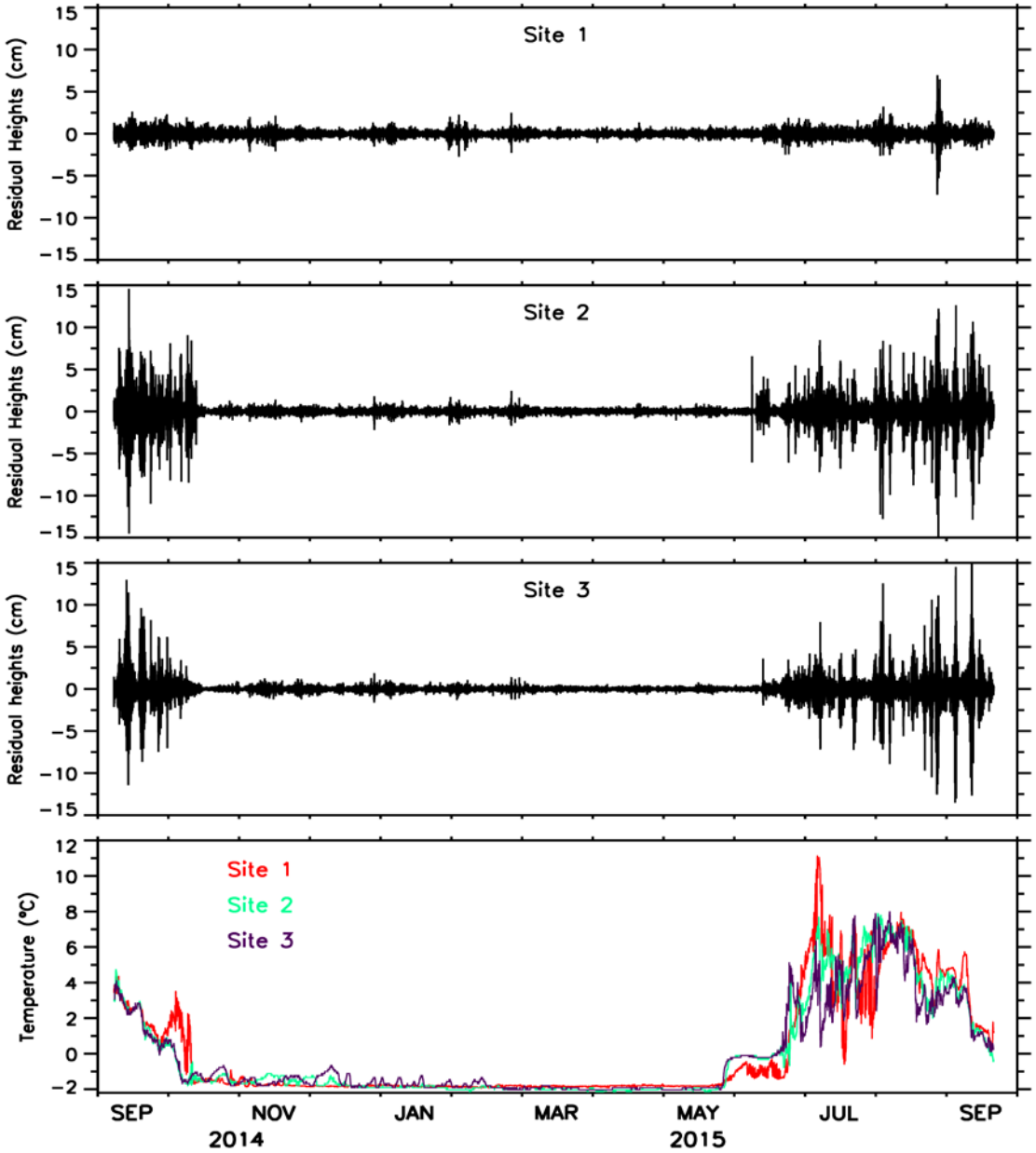

Figure 5: Year-long time series of sea level height residuals (top three panels) and temperatures (bottom panel) at the three Elson Lagoon sites.

Tidal Height Anomalies

Thirty-seven standard tidal constituents were fit to the sea level heights at Red Dog, Elson Lagoon, and Prudhoe Bay using a least squares procedure. The resulting composite tidal height anomalies, overlaid with the combined solar semi-annual (SSA) and solar annual (SA) constituent signal, are shown in Figure 6. Corresponding amplitudes and phases for all 37 tidal constituents are listed in Table 2. The long-period SSA+SA signal generally exhibits a winter minimum (negative anomaly) from October through mid-May and summer maximum (positive anomaly) from mid-May through September, suggesting that this long-period signal might not be tidal; rather, it may be related to seasonal changes in large-scale ocean circulation.

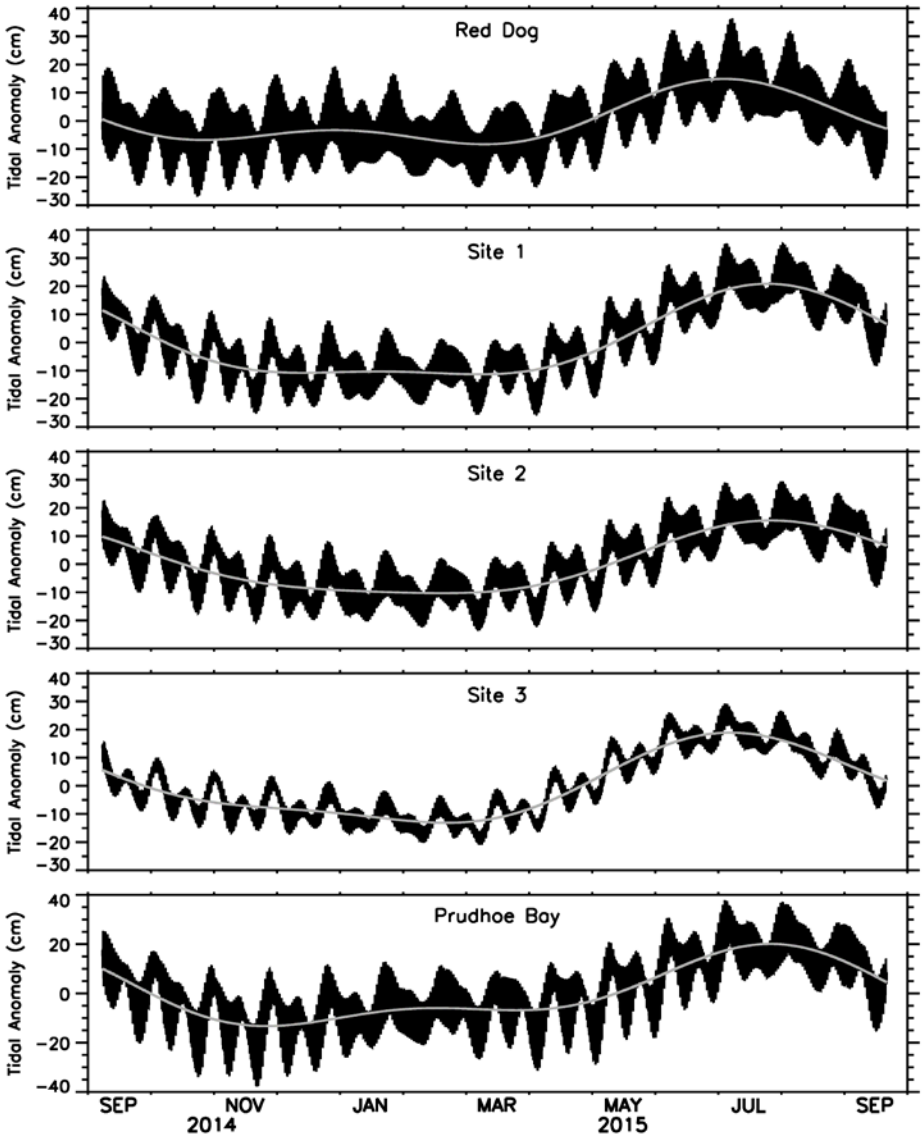

Figure 6: Year-long time series of 37-constituent composite tidal height anomalies at Red Dog dock, Elson Lagoon sites, and Prudhoe Bay (black). The white lines show the combined solar semi-annual solar (SSA) and solar annual (SA) signal.

Table 2 results show that the M2 tide is the largest of the semidiurnal signals at all five locations. Furthermore, the largest M2 tides occur at Red Dog and Prudhoe Bay and the smallest at Elson Lagoon Site 3. These M2 characteristics can also be inferred from the envelope widths of the composite tidal signals shown in Figure 6.

Table 2: Amplitudes (cm) and phases (degrees) of the 37 standard tidal constituents at Red Dog dock, Elson Lagoon sites, and Prudhoe Bay. Phases are relative to 0000 UTC, 1 January 2014.

		RED DOG		SITE 1		SITE 2		SITE 3		PRUDHOE BAY	
		AMP	PHASE	AMP	PHASE	AMP	PHASE	AMP	PHASE	AMP	PHASE
1	M2	8.63	90.9	4.77	73.8	4.65	66.0	2.22	63.3	6.74	93.6
2	S2	1.62	22.0	2.00	15.2	1.92	8.5	0.89	9.5	3.12	45.3
3	N2	1.76	176.8	0.70	116.1	0.76	115.9	0.37	106.1	0.89	129.8
4	K1	1.97	309.6	1.84	207.7	1.87	202.7	1.08	186.6	2.21	214.9
5	M4	0.18	280.5	0.09	65.5	0.03	224.5	0.03	152.4	0.08	294.3
6	O1	0.65	165.7	1.29	190.6	1.32	185.2	0.81	173.7	2.87	166.9
7	M6	0.08	103.3	0.02	178.8	0.04	130.7	0.01	51.5	0.03	65.3
8	MK3	0.23	315.4	0.03	201.0	0.06	139.9	0.02	155.1	0.08	147.8
9	S4	0.01	121.3	0.04	139.7	0.04	78.3	0.03	45.8	0.06	249.0
10	MN4	0.12	345.4	0.01	181.6	0.05	303.1	0.03	255.3	0.06	318.8
11	NU2	0.05	113.6	0.14	57.9	0.13	62.6	0.04	33.5	0.23	135.5
12	S6	0.04	214.3	0.02	129.5	0.03	148.0	0.04	134.3	0.02	138.8
13	MU2	0.27	342.8	0.05	15.7	0.10	319.2	0.05	153.5	0.23	83.8
14	2N2	0.49	229.7	0.10	143.4	0.08	110.3	0.01	88.7	0.15	239.6
15	OO1	0.40	128.0	0.10	33.7	0.09	325.3	0.05	250.4	0.06	299.9
16	LAM2	0.13	237.9	0.08	177.4	0.17	152.9	0.09	117.0	0.22	296.3
17	S1	1.19	232.0	0.30	103.5	0.24	100.2	0.19	45.5	0.47	257.9
18	M1	0.13	61.9	0.27	225.4	0.17	226.7	0.07	224.8	0.26	198.5
19	J1	0.46	197.9	0.12	246.5	0.12	253.0	0.12	213.8	0.36	184.1
20	MM	4.12	311.2	4.91	321.9	4.72	322.0	3.63	341.3	5.51	325.2
21	SSA	5.77	359.8	5.26	316.4	2.79	318.8	4.50	5.8	6.73	301.7
22	SA	9.15	174.7	15.60	156.8	12.76	153.0	14.74	166.2	13.70	166.6
23	MSF	3.47	174.5	3.43	178.3	2.58	171.3	1.90	133.8	4.29	176.6
24	MF	2.75	261.0	3.89	289.1	3.78	287.8	3.62	266.1	5.90	282.8
25	RHO	0.20	188.1	0.03	302.6	0.02	248.1	0.03	276.8	0.18	215.2
26	Q1	0.43	256.7	0.44	189.0	0.43	182.8	0.30	178.8	0.88	192.6
27	T2	0.46	302.5	0.59	300.8	0.71	308.4	0.46	303.3	0.27	42.7
28	R2	0.85	175.7	0.46	170.2	0.52	174.7	0.37	153.0	0.16	169.0
29	2Q1	0.35	266.8	0.16	165.9	0.21	170.6	0.16	138.3	0.28	304.6
30	P1	0.58	285.4	0.86	181.0	0.80	179.6	0.49	182.6	0.95	161.9
31	2SM2	0.15	138.8	0.12	120.9	0.17	116.9	0.10	106.1	0.17	85.4
32	M3	0.05	15.1	0.01	256.5	0.05	229.1	0.01	229.0	0.02	267.9
33	L2	0.28	205.0	0.15	266.2	0.16	269.2	0.10	314.4	0.29	221.8
34	2MK3	0.17	50.4	0.02	138.6	0.05	14.6	0.01	50.4	0.06	64.7
35	K2	0.71	260.6	0.37	279.2	0.29	278.2	0.17	291.3	0.69	214.8
36	M8	0.03	204.2	0	34.7	0.02	272.9	0.01	18.1	0.02	342.4
37	MS4	0.03	210.5	0.05	16.3	0.06	156.0	0.05	108.3	0.06	273.7

The Site 1 amplitudes for the M2, S2, and N2 constituents (4.77 cm, 2.00 cm, and 0.70 cm, respectively) are all less than the corresponding amplitudes for these constituents (6.0 cm, 3.4 cm, and 3.4 cm) estimated by Okkonen (2008) from a 22-day, 2006 late summer, open-water deployment at a nearby (~440 m distant) location. Given the different deployment periods for the present study and the 2008 study, it is possible the different study results might be attributable, in part, to seasonal attenuation of the semidiurnal signal by sea ice. This notion was investigated by using a least squares procedure to repetitively fit M2, S2, and N2 sinusoids to 30-day sea level time series, advanced sequentially in one-day increments. The results of this exercise (Figure 7) show that the amplitudes of these semidiurnal signals are generally larger during the open-water months (July–September) than during the ice-covered months (November–May), with the most prominent amplitude changes occurring during freeze-up (October) and breakup (June). The companion phase plots show that the phase differences between sites are very small during the open-water months but increase as winter progresses and as sea ice (presumably) grows thicker. In April and May, the phase differences between Sites 1 and 3 for the M2 and S2 tides have reached their maxima (~40 degrees). In other words, the M2 and S2 tides take ~80 minutes longer to propagate from Site 1 to Site 3 at the end of the ice growing season than during the open water season.

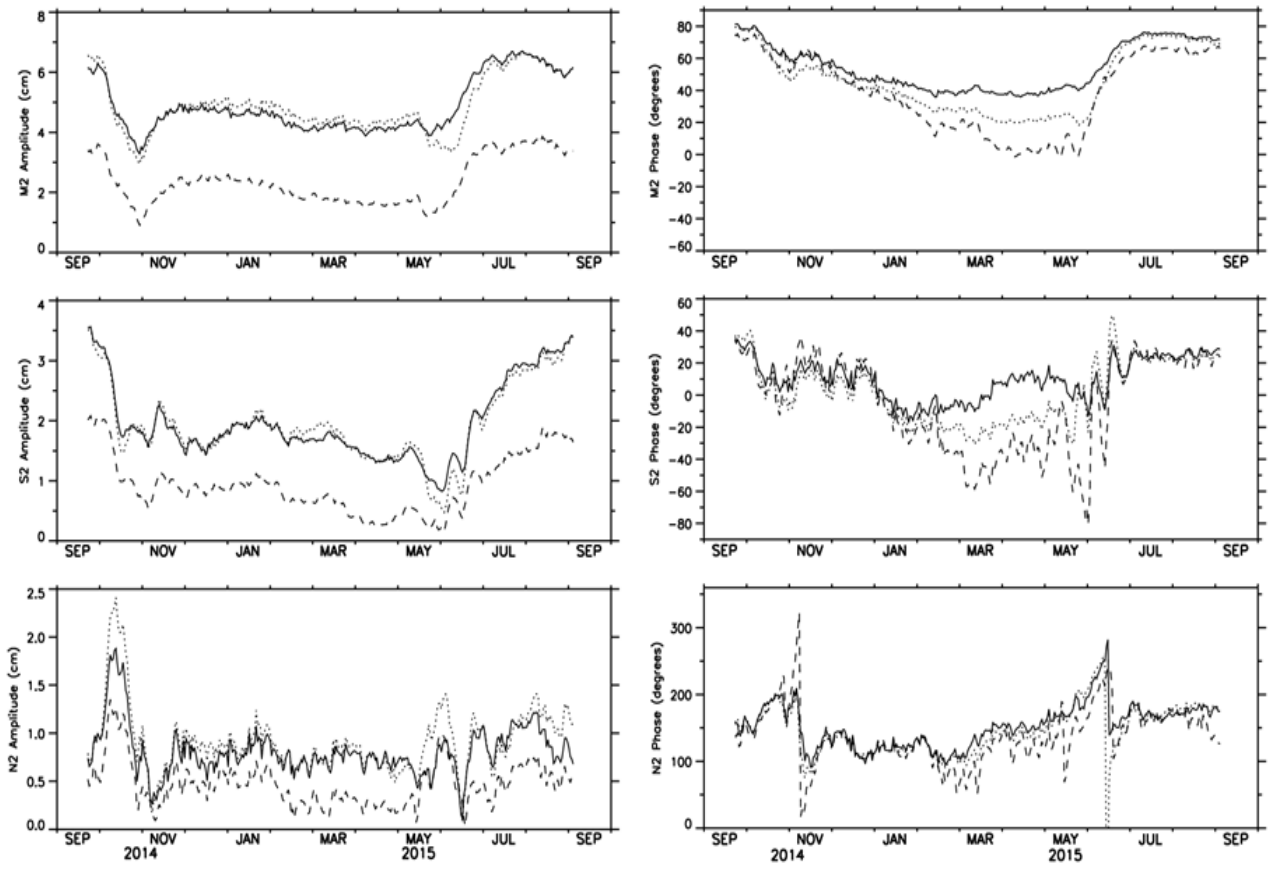

Figure 7: Seasonal variations of semidiurnal tidal amplitudes (left panels) and phases (right panels) at Elson Lagoon (Site 1 - solid, Site 2 - dot, and Site 3 - dash).

Non-Tidal Height Anomalies

Non-tidal height anomalies at Red Dog, Elson Lagoon, and Prudhoe Bay appear to be generally coherent (Figure 8). Statistically significant cross-correlation coefficients for paired 378-day time series (Table 3) support this inference. Correlations between heights at a given site and sites downstream (in a Kelvin wave sense) diminish and lags increase with increasing distance between sites, which is consistent with an interpretation that these sea level anomalies are associated with shelf waves generated in the Bering Sea and/or southern Chukchi Sea (Danielson et al., 2014). The lag results (Table 3) indicate that representative shelf wave signals take ~23 hours to propagate the ~950 km from Red Dog dock to Prudhoe Bay, a phase speed of ~990 km d^{-1} (11.5 m s^{-1}), while comparison of representative anomaly amplitudes at Red Dog and Prudhoe Bay (27 cm S.D. and 17 cm S.D., respectively; Figure 8) indicates that these propagating signals are markedly attenuated over this distance. Even during the winter months, when there is a canopy of landfast sea ice above nearshore waters, non-tidal sea level anomalies of +/- 25 cm propagate along the Chukchi and Beaufort coasts.

Non-local forcing of these apparent shelf waves can also be inferred from plots comparing lagged correlations between coastal non-tidal sea level and winds (projected along the principal axis of variance) at each NCEP grid point across the Bering-Chukchi-Beaufort region. Figure 9 (top panel) shows that non-tidal sea level at Red Dog is well-correlated with generally meridional winds extending from the southcentral Bering Sea through Bering Strait and into the southern Chukchi Sea. The positive correlation coefficient means that winds from the south will raise Red Dog sea level while winds from the north will lower sea level. The maximum correlation (r = 0.62) is for winds (projected along 3°T–183°T) at 65°N, 167.5°W leading Red Dog sea level by ~18 hours (Figure 9, bottom panel). Similarly, Elson Lagoon Site 2 non-tidal sea level anomalies are well-correlated with meridional and southwesterly-northeasterly winds extending from southcentral Bering Sea through Bering Strait and into the eastern Chukchi Sea (Figure 10, top panel). Elson Lagoon sea level is best correlated (r = 0.62) with winds (projected along 52°T–232°T) at 70°N, 167.5°W and leading Elson Lagoon sea level by ~6 hours (Figure 10, bottom panel). Results for Elson Lagoon Sites 1 and 3 are very similar to Site 2 results and are not shown here. Figure 11 shows that non-tidal sea level at Prudhoe Bay is well-correlated with southwesterly and northeasterly winds in the northeastern Chukchi Sea and western Beaufort Sea, but not with winds further south. For sea level at all five recording sites, winds upstream of the recording sites provide the best correlations. Moreover, changes in upstream winds occur many hours before corresponding changes in sea level are observed. Both of these conditions support the notion that remotely forced shelf waves represent a significant contribution to non-tidal sea level along the Alaskan Chukchi and Beaufort coasts.

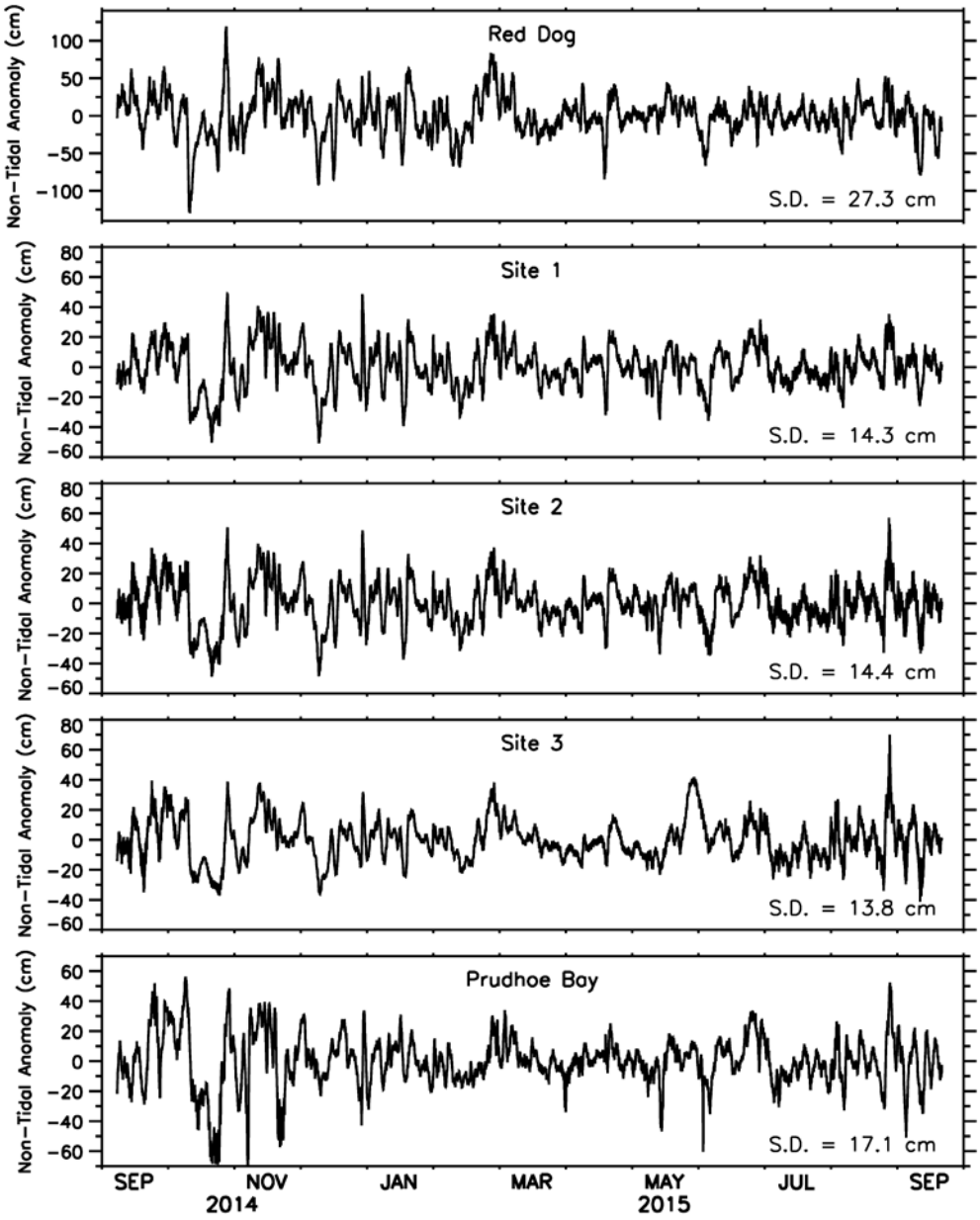

Figure 8: Year-long time series of non-tidal height anomalies at Red Dog dock, Elson Lagoon sites (Site 1–3), and Prudhoe Bay. Each plot is annotated with the standard deviation (S.D.) of its anomaly time series. Note that the anomaly height scales differ from plot to plot.

Table 3: Lagged cross-correlations between non-tidal sea level anomalies. All correlations are significant at $p < 0.01$ for 31 effective degrees of freedom based on a decorrelation time scale of 12 days (378 days / 12 days = 31.5 df).

	Site 1	Site 2	Site 3	Prudhoe Bay
Red Dog	0.80 (11.5 hr)	0.78 (12.0 hr)	0.67 (15.5 hr)	0.53 (23.0 hr)
Site 1		0.98 (0.5 hr)	0.82 (3.5 hr)	0.76 (11.5 hr)
Site 2			0.87 (2.5 hr)	0.79 (10.5 hr)
Site 3				0.75 (7.0 hr)

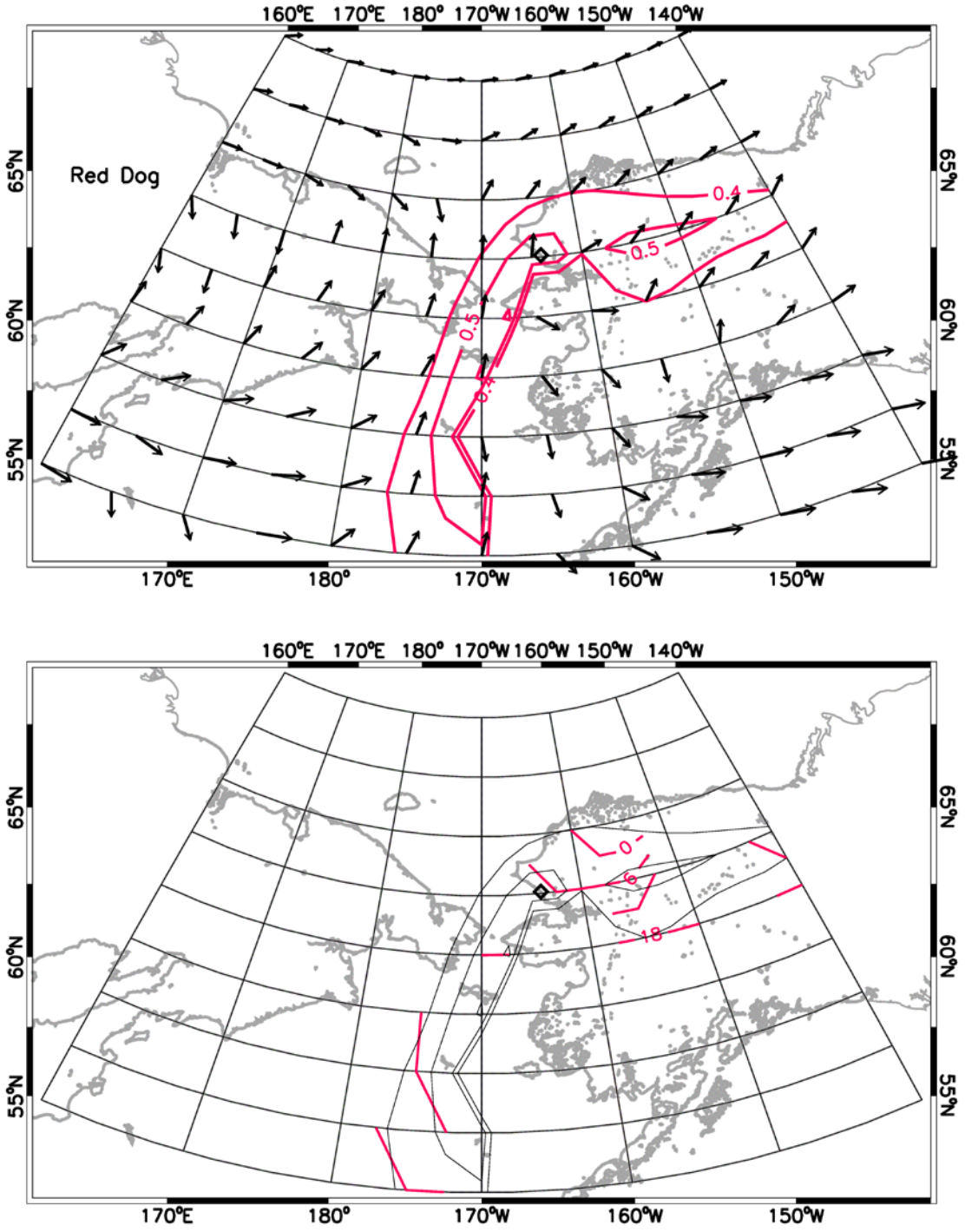

Figure 9: Cross-correlation (top panel; red contours) between winds projected along their axes of variance (top panel; black arrows) and non-tidal sea level at Red Dog dock (black diamond). $r > 0.4$ is significant at $p<0.05$ based on 16 effective degrees of freedom; 23-day decorrelation time scale, 378-day time series. Red contours in bottom panel indicate lags (hours) within the region where correlations are statistically significant. Wind leads sea level for positive lags.

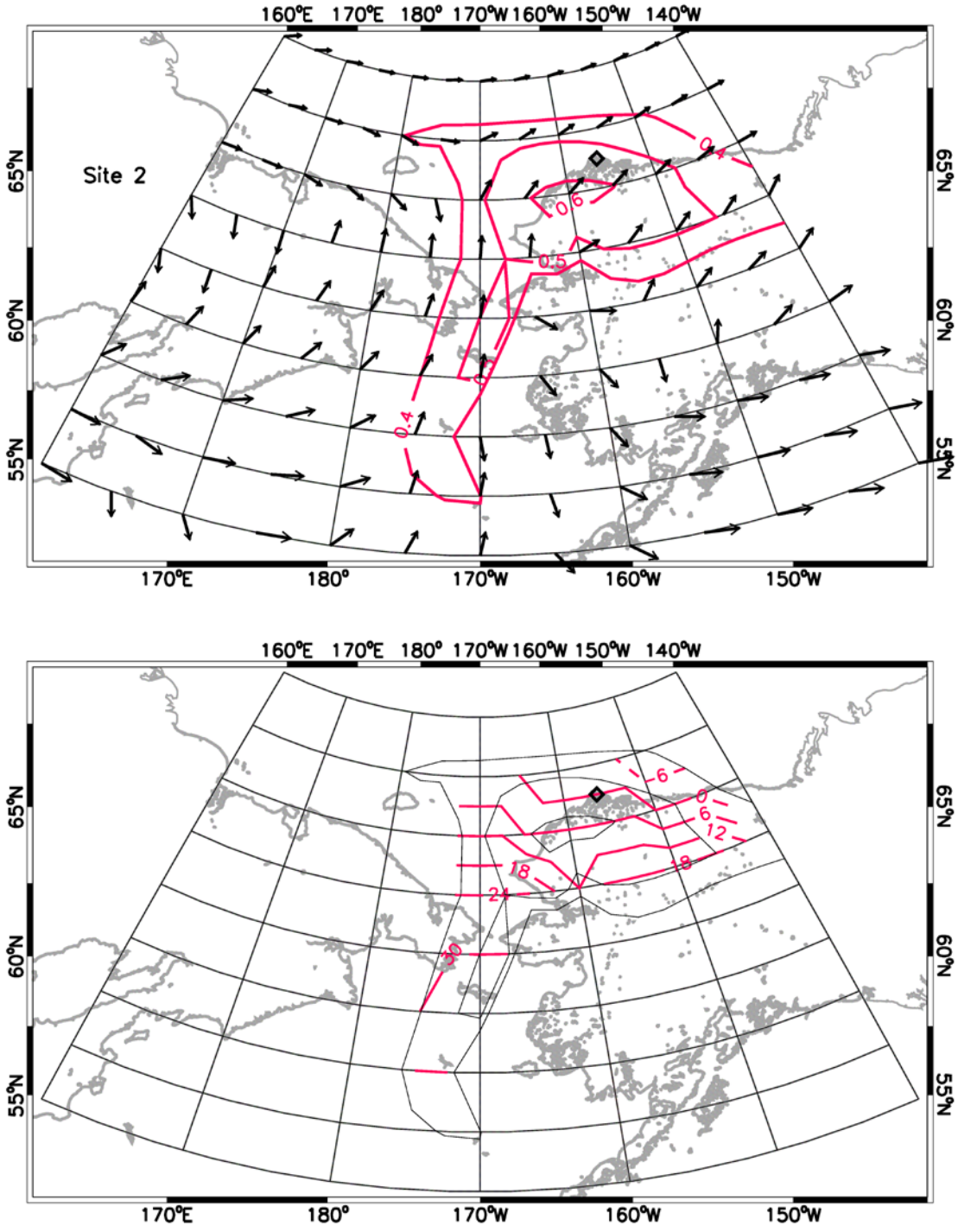

Figure 10: Cross-correlation (top panel; red contours) between winds projected along their axes of variance (top panel; black arrows) and non-tidal sea level at Elson Lagoon Site 2 (black diamond). $r > 0.4$ is significant at $p<0.05$ based on 16 effective degrees of freedom; 23-day decorrelation time scale, 378-day time series. Red contours in bottom panel indicate lags (hours) within the region where correlations are statistically significant. Wind leads sea level for positive lags.

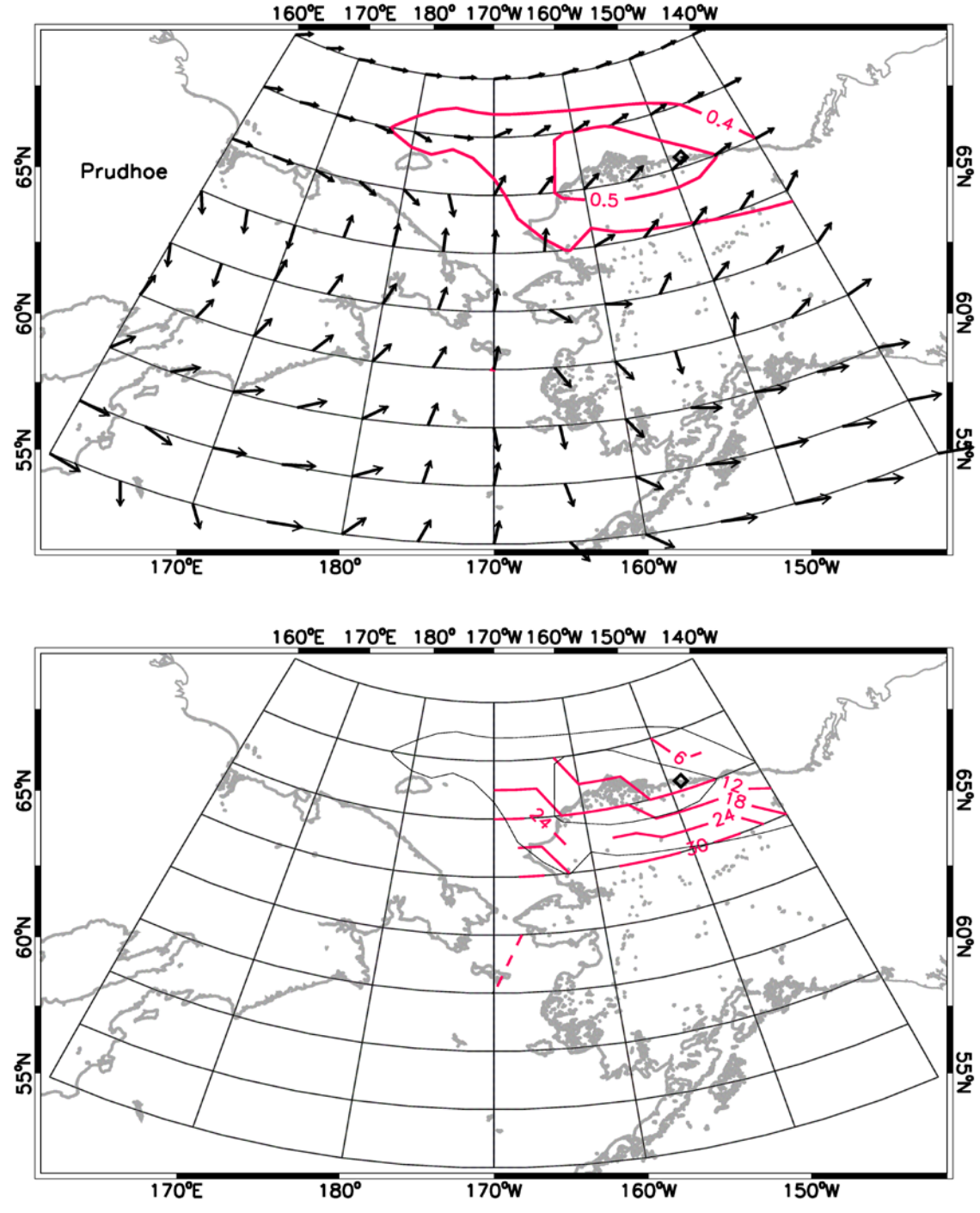

Figure 11: Cross-correlation (top panel; red contours) between winds projected along their axes of variance (top panel; black arrows) and non-tidal sea level at Prudhoe Bay (black diamond). $r > 0.4$ is significant at $p<0.05$ based on 16 effective degrees of freedom; 23-day decorrelation time scale, 378-day time series. Red contours in bottom panel indicate lags (hours) within the region where correlations are statistically significant. Wind leads sea level for positive lags.

Some aspects of seasonality of non-tidal sea level can be also be ascertained from cross-correlation analyses. Lagged correlations between Red Dog and Prudhoe Bay sea level for fall open-water, winter ice-covered, and summer open-water periods (Table 4) are similar across seasons suggesting that shelf wave propagation along the Chukchi and Beaufort coasts is not greatly impacted by sea ice cover. However, within Elson Lagoon, comparison of seasonal lagged correlations between non-tidal height anomalies at Sites 1 and 3 suggest that signals traveling the 34-km distance between these two sites are attenuated and perhaps scattered (smaller correlation coefficient) and are significantly slowed (larger lag) during the winter ice-covered period. Based on the phase lags and distance between Sites 1 and 3 (Table 4), the phase speed is 2.1 m s^{-1} under ice, whereas the phase speed is 4.7–6.3 m s^{-1} in open water. The simplest explanation for the marked seasonal differences in phase speeds would be due to seasonal differences in (liquid) water depth. Wave speed, *c*, in shallow water of depth *h* is given by:

$$c = \sqrt{gh}$$ in which g is gravitational acceleration. Equation 4

Based on the above phase speeds, a representative depth for the open-water periods is between ~2.25–4.0 m. The deployment depths of the Elson moorings (see Methods) very nearly reside within this depth range. The water depth corresponding to the 2.1 m s^{-1} wave speed during the winter period is 0.45 m. At first consideration, a winter water depth of 0.45 m (a ~45 hPa pressure equivalent) would appear to be an error. However, adding a pressure contribution from ~1.5–2 m of overlying sea ice (~135–180 hPa) would result in a measured bottom pressure of 180–225 hPa (equivalent water depth of ~1.8–2.25 m). This result implies that the winter anomalies depicted in Figure 8 also represent changes in sea ice elevation that, given the plastic nature of sea ice, potentially introduce or aggravate stress fractures within the ice.

Table 4: Seasonal lagged cross-correlations between non-tidal sea level anomalies. Fall (8 Sep 2014–13 Oct 2014); Winter (14 Oct 2014–13 Jun 2015); Summer (14 Jun 2015–20 Sep 2015). Based on a decorrelation time scale of 12 days, the Fall, Winter and Summer seasons are characterized by 3, 20 and 8 degrees of freedom, respectively. Fall correlations are not significant at $p<0.05$. Winter correlations are all significant at $p<0.01$. Summer correlations are all significant at $p<0.05$.

		Site 1	Site 2	Site 3	Prudhoe Bay
	F	0.83 (11.5 hr)	0.79 (12.5 hr)	0.70 (14.5 hr)	0.49 (23.5 hr)
Red Dog	W	0.81 (11.0 hr)	0.81 (11.5 hr)	0.67 (15.5 hr)	0.53 (22.5 hr)
	S	0.69 (11.5 hr)	0.66 (12.5 hr)	0.62 (14.5 hr)	0.53 (23.5 hr)
	F		0.97 (0.0 hr)	0.91 (1.5 hr)	0.75 (12.5 hr)
Site 1	W		0.99 (0.5 hr)	0.80 (4.5 hr)	0.76 (11.5 hr)
	S		0.95 (0.5 hr)	0.86 (2.0 hr)	0.79 (10.5 hr)
	F			0.94 (0.5 hr)	0.79 (10.0 hr)
Site 2	W			0.84 (3.0 hr)	0.76 (10.5 hr)
	S			0.91 (1.0 hr)	0.87 (9.5 hr)
	F				0.87 (8.0 hr)
Site 3	W				0.68 (6.0 hr)
	S				0.88 (7.5 hr)

Elson Lagoon Sea Level and Meade River Freshet

As mentioned above, non-tidal height anomalies are largely coherent along the Chukchi and Beaufort coasts. However, closer inspection of non-tidal sea level at the three Elson Lagoon sites indicates that, from ~26 May to 7–8 June 2015, the sea level anomaly at Site 3 was ~30 cm greater than at Sites 1 and 2 (top panel, Figure 12). Coincidentally, the temperature jumped from ~ -1.8°C to ~0.0°C, first at Site 3 on ~27–29 May 2015 and then a day or so later at Site 2, signaling the arrival of the spring freshet at these mooring locations (middle panel, Figure 12). The short-duration hydrograph for the Meade River, which discharges into the southern end of Admiralty Bay, indicates that the freshet was waning by the time the freshwater signal traveled from the river mouth to Sites 2 and 3. Temperature increased much more slowly at Site 1, reaching a local maximum of -0.41°C on 6 June.

Residual sea levels at Site 2 increased from < 1 cm to > 2 cm on ~11 June while residuals at Site 3 increased to >2 cm on ~14 June (bottom panel, Figure 12), suggesting that sea ice became sufficiently thin to admit high frequency surface waves and thereby identify the onset of breakup. The residual spike on 9 June is an artifact of the 3-point smoothing.

Because Site 3 is closer to the mouth of the Meade River, the sea ice at the eastern end of Elson Lagoon is likely less saline and therefore has a slightly higher latent heat of fusion than sea ice at Sites 1 and 2. Given that the water temperatures at Sites 2 and 3 are similar, the more saline ice at Site 2 should melt before less saline ice at Site 3.

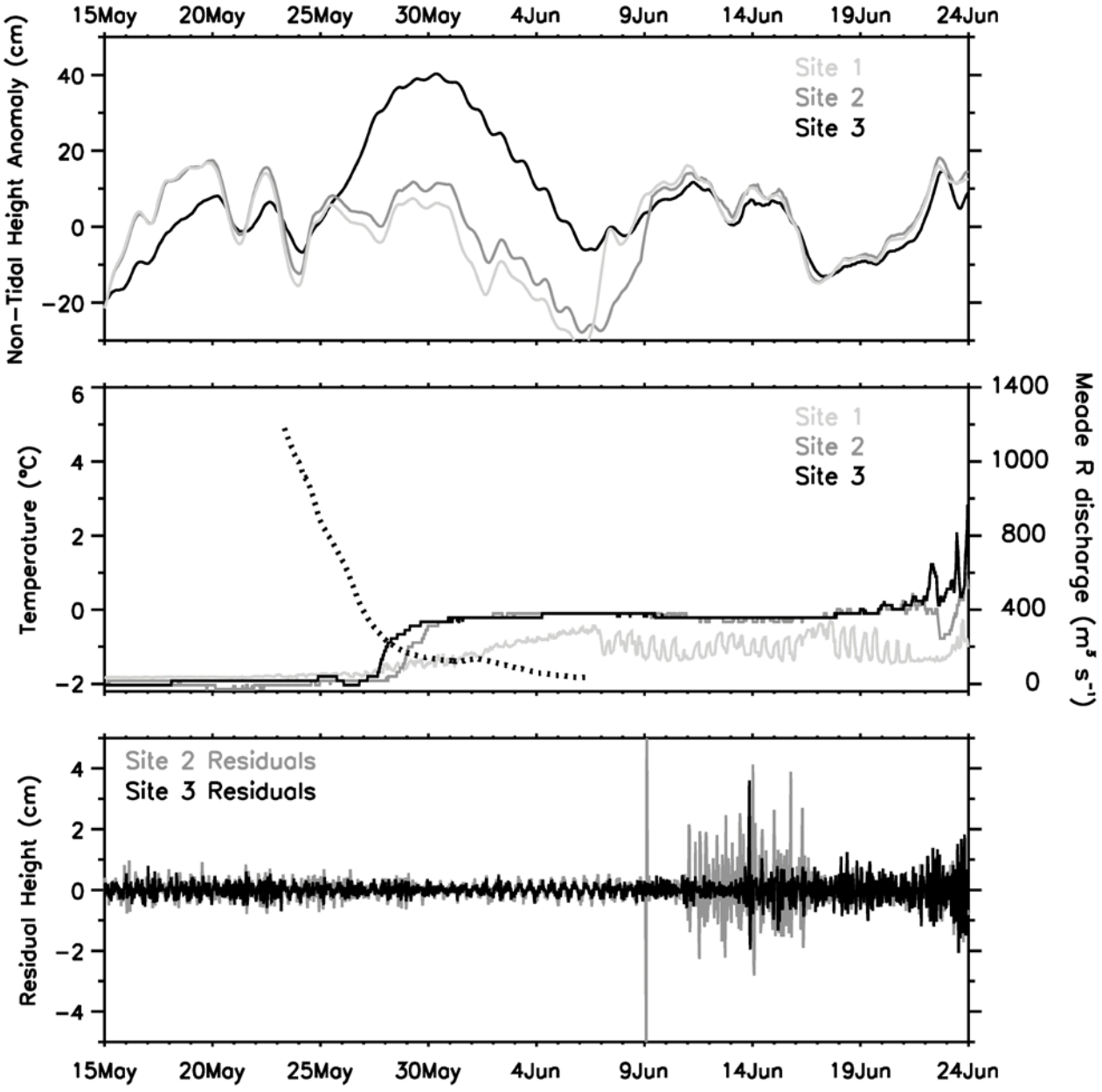

Figure 12: Meade River discharge (middle panel; dotted line) and Elson Lagoon non-tidal sea level anomalies (top panel), bottom temperatures at moorings (middle panel; solid lines), and residual heights (bottom panel).

CONCLUSIONS

Year-long records of sea level derived from pressure sensor moorings in Elson Lagoon near Barrow, Alaska were analyzed with companion sea level records acquired by NOAA tide gauges at Red Dog dock and Prudhoe Bay. The presence of landfast sea ice impacts both tidal and non-tidal sea level signals.

In Elson Lagoon, the amplitudes of the semidiurnal tides (M2, S2, and N2) are larger during the open-water season (mid-June to mid-October) than during the ice-covered season (mid-October to mid-June). The associated phases of the semidiurnal tides are very similar at the three Elson Lagoon sites during the open-water season, but phase differences increase as winter progresses and as sea ice grows thicker.

Non-tidal sea level signals are coherent from Red Dog dock along the southern Alaskan Chukchi coast to at least Prudhoe Bay along the central Alaskan Beaufort coast, a coastwise distance of ~950 km. These non-tidal signals are characteristic of shelf waves that are likely generated by winds in the Bering and Chukchi Seas. The speed at which these signals propagate along the coast does not exhibit much seasonal variability. However, the presence of ice cover significantly slows the propagation of non-tidal signals within Elson Lagoon. The slow propagation speed implies a very shallow layer of water (perhaps less than 1 m) beneath the ice by late winter.

Breakup in Elson Lagoon follows the Meade River spring freshet. An apparent sea level bulge at the eastern end of Elson Lagoon in late May and early June suggests that Admiralty Bay-Dease Inlet can act as a temporary reservoir for the freshet.

ACKNOWLEDGEMENTS

Pete Shipton, University of Alaska Fairbanks, developed the simple, functional, and effective design for the moorings. Billy Adams, North Slope Borough Department of Wildlife Management, deployed and recovered the Elson Lagoon moorings. This research was supported by the University of Alaska Fairbanks Coastal Marine Institute, BOEM (cooperative agreement M14AC00016), and the North Slope Borough/Shell Baseline Studies Research Agreement.

STUDY PRODUCTS

Okkonen, S.R. 2015. Sea Level Measurements along the Alaskan Chukchi and Beaufort Coasts. Oral presentation. University of Alaska Coastal Marine Institute Annual Research Review, January 2015, Anchorage, Alaska.

Okkonen, S.R. 2016. Sea Level Measurements along the Alaskan Chukchi and Beaufort Coasts. Poster presentation. Alaska Marine Science Symposium, January 2016, Anchorage, Alaska.

Okkonen, S.R. 2016. Sea Level Measurements along the Alaskan Chukchi and Beaufort Coasts. Oral presentation. University of Alaska Coastal Marine Institute Annual Research Review, January 2016, Anchorage, Alaska.

Okkonen, S.R. 2016. Sea Level Measurements along the Alaskan Chukchi and Beaufort Coasts. Final Report. OCS Study 2016-075. University of Alaska Coastal Marine Institute, University of Alaska Fairbanks and USDOI BOEM, Alaska OCS Region.

Okkonen, S.R. and T. Sformo. 2017. Relationships among sea level, hydrography and circulation in coastal waters near Barrow, Alaska. Poster presentation. Alaska Marine Science Symposium, January 2017, Anchorage, Alaska.

REFERENCES

Danielson, S.L., T.J. Weingartner, K.S. Hedstrom, K. Aagard, R. Woodgate, E. Chuchister, and P.J. Stabeno. 2014. Coupled wind-forced controls of the Bering-Chukchi shelf circulation and the Bering Strait throughflow: Ekman transport, continental shelf waves, and variations of the Pacific-Arctic Sea surface height gradient. Prog. Oceanogr., 125:40–61.

Johnson, M.A., H. Eicken, M.L. Druckenmiller, and R. Glenn, Editors. 2014. Experts Workshop to Comparatively Evaluate Coastal Currents and Ice Movement in the Northeastern Chukchi Sea; Barrow and Wainwright, Alaska, March 11–15, 2013. University of Alaska Fairbanks, Fairbanks, Alaska. 48 pp.

Okkonen, S.R. 2008. Exchange between Elson Lagoon and the near shore Beaufort Sea and its role in the aggregation of zooplankton. Final Report. OCS Study MMS 2008-010, US Department of the Interior, Minerals Management Service, Alaska OCS Region, 18 pp.

The Department of the Interior Mission

As the Nation's principal conservation agency, the Department of the Interior has responsibility for most of our nationally owned public lands and natural resources. This includes fostering the sound use of our land and water resources, protecting our fish, wildlife and biological diversity; preserving the environmental and cultural values of our national parks and historical places; and providing for the enjoyment of life through outdoor recreation.The Department assesses our energy and mineral resources andworks to ensure that their development is in the best interests of all our people by encouraging stewardship and citizen participation in their care. The Department also has a major responsibility for American Indian reservation communities and for people who live in island communities.

The Bureau of Ocean Energy Management

The Bureau of Ocean Energy Management (BOEM) works to manage the exploration and development of the nation's offshore resources in a way that appropriately balances economic development, energy independence, and environmental protection through oil and gas leases, renewable energy development and environmental reviews and studies.